applied sciences

MDPI

Article

A Low-Profile Ferrite Dipole VHF Antenna for Integrated Mast Applications

Won Bin Park [1], Son Trinh-Van [1], Youngoo Yang [1], Kang-Yoon Lee [1], Byunggil Yu [2], Jinwoo Park [2], Hojeong You [3] and Keum Cheol Hwang [1,*]

[1] Department of Electrical and Computer Engineering, Sungkyunkwan University, Suwon 440-746, Korea; wonbin923@hanmail.net (W.B.P.); jsonbkhn@gmail.com (S.T.-V.); yang09@skku.edu (Y.Y.); klee@skku.edu (K.-Y.L.)

[2] Tactical Communication. Team, Hanwha Systems, Seongnam 13524, Korea; byunggil77.yu@hanwha.com (B.Y.); jw0822.park@hanwha.com (J.P.)

[3] Naval Systems. 1st Team, Hanwha Systems, Gumi 39376, Korea; hj8251.you@hanwha.com

* Correspondence: khwang@skku.edu; Tel.: +82-31-290-7978

Received:13 January 2020; Accepted:13 February 2020; Published: 1 March 2020

Abstract: In this paper, an extremely low-profile ferrite dipole antenna operating on the VHF band (30–300 MHz) is proposed. The design antenna consists of 44 plate-type ferrite cells arranged into two stacked ferrite layers: a bottom ferrite layer with 2×12 grid cells and a top ferrite layer with 2×10 grid cells. The antenna is excited by an electric loop feeding structure and maximum gain performance is achieved when the loop feeding structure has five loops. To validate the performance of the proposed antenna, an antenna prototype is fabricated and tested at an outdoor range. The antenna weighs 1.45 kg and has electrical dimensions of approximately $0.0636 \times 0.0112 \times 0.0008\lambda_L^3$ at the lowest operating frequency of 30 MHz. The measured realized gain varies from -31.48 to -2.44 dBi within the VHF band. Reasonable agreement is also obtained between the measurement and simulation results. To assess the performance of the proposed antenna, it was mounted on the integrated mast of an offshore patrol vessel (OPV) model. The antenna on the OPV was also simulated and the results discussed.

Keywords: dipole antenna; ferrite; integrated mast; loop feed; offshore patrol vessel; VHF

1. Introduction

Modern naval warships carry out various operations at sea, including responding to multiple threats, such as anti-ship, anti-aircraft, anti-submarine, and land threats; securing maritime control; and securing maritime transportation routes. A multitude of antennas for communication, navigation, electronic warfare, and radar are separately mounted on warships to ensure their smooth operation. An increase in the number of antennas reduces the survivability of warships due to the high radar cross section (RCS) and degrades the performance capabilities of the systems due to electromagnetic interference (EMI). Recently, the concept of an integrated mast was introduced to overcome the RCS and EMI problems [1–4]. An integrated mast can reduce RCS and EMI structurally through the use of a radome with a frequency selective surface [5,6]. However, traditional monopole antennas of the types widely used on warships have several disadvantages when mounted on the face of an integrated mast, such as their high-profile and weight issues [7–10]. Various antennas have been developed to realize low-profile [11–20]. For low-profile, the antenna is designed as a loop-type structure or with high permittivity and/or permeability materials. For example, four half loops with a bent diamond structure placed on the ground were designed with a height of $0.116\lambda_L$ at the lowest operating frequency [16]. In another study [17], a monopole shaped bow-tie antenna with two top hats, two shorting pins, and a ring slot cut into the ground plane was designed with a height of $0.085\lambda_L$. Several ferrite structures effectively applied to the inside of a loop radiator were introduced to realize low-profile design with a height of $0.00508\lambda_L$ [18]. In other work [19], a conformal ferrite dipole antenna with an electrically separated four-loop feeding structure was suggested, showing a very low-profile with a height of $0.00381\lambda_L$.

In this paper, an extremely low-profile ferrite dipole VHF antenna with a height of only $0.0008\lambda_L$ is proposed for application to an integrated mast. To ensure the minimal size and weight of the antenna, 44 plate-type ferrite cells with a total weight of approximately 1.45 kg are used with the ferrite dipole antenna. The antenna is fed by an electric loop feeding structure. By applying a loop feeding structure with five loops, the magnetic distribution is changed from a triangular distribution to a quasi-uniform distribution. As a result, the gain of the antenna in the high frequency band is significantly improved. In the following sections, details of the design and performance of the proposed antenna are presented and discussed. The proposed antenna when mounted on the integrated mast of the offshore patrol vessel (OPV) is also examined.

2. Antenna Design

Figure 1a presents an illustration of the 3-D view of the proposed antenna, which consists of a ferrite dipole, a ground plane, and a loop-type feeding structure. The overall size of the ferrite dipole is $0.0636 \times 0.0106 \times 0.0005\lambda_L^3$ at the lowest operating frequency. The ferrite geometry consists of 44 plate-type ferrite cells (MP2106-0M0, Laird [21]) arranged into two stacked arrays—one with 2×12 grid cells on the bottom and one with 2×10 grid cells on the top—as shown in Figure 1a. The dimensions of each cell are $L_f \times L_f \times H_f$. Figure 1b presents the feeding structure, which consists of two long microstrip lines at the center, ten short microstrip lines, and a coaxial probe. Two long microstrip lines $L_1 \times W_2$ in size are separated by a distance of d_3. Each short microstrip line is $W_1 \times (L_2 + L_3)$ in size with one end connected to the long microstrip line and the other end connected to the ground plane. A pair of short microstrip lines on both sides forms a one-quarter rectangular loop, and there are five one-quarter rectangular loops in total wrapped around the ferrite. The feeding structure is designed using copper tape on Styrofoam; it has a relative dielectric constant of 1.03, a loss tangent of 0.0001, and a thickness of 3 mm. The Styrofoam is directly placed on top of the ferrite cells. A coaxial probe is used to feed the ferrite antenna, and the inner and outer conductors of the coaxial probe are connected to the upper and lower arms of the one-quarter rectangular loop located at the center. The design parameters of the proposed antenna are optimized to ensure high gain performance, and the optimized values are summarized in Table 1.

Table 1. Optimized dimensional parameters of the proposed antenna.

Parameter	Value	Parameter	Value
L_1	487 mm	W_1	10 mm
L_2	55 mm	W_2	2 mm
L_3	8 mm	d_1	101.3 mm
L_f	53 mm	d_2	117.2 mm
H_f	2.5 mm	d_3	2 mm

The complex permeability and magnetic loss tangent properties of the MP2106-0M0 ferrite are shown in Figure 2. The complex permeability consists of a real part μ' and an imaginary part μ''. The magnetic loss tangent of the ferrite is calculated as μ''/μ'. The permittivity value of the ferrite is set to 12 in the operating frequency band (from 30 MHz to 300 MHz). As observed in Figure 2, the μ'-value of MP2106-0M0 is high in the low frequency band, and the magnetic loss tangent increases sharply as the frequency increases. For magnetic dipole applications, high radiation efficiency can be obtained with a high μ'. Unlike a dielectric resonator antenna, the high magnetic loss tangent does not degrade the radiation efficiency of the magnetic resonator [19]. Therefore, the ferrite MP2106-0M0 is useful in the design of a magnetic dipole antenna operating on the VHF band.

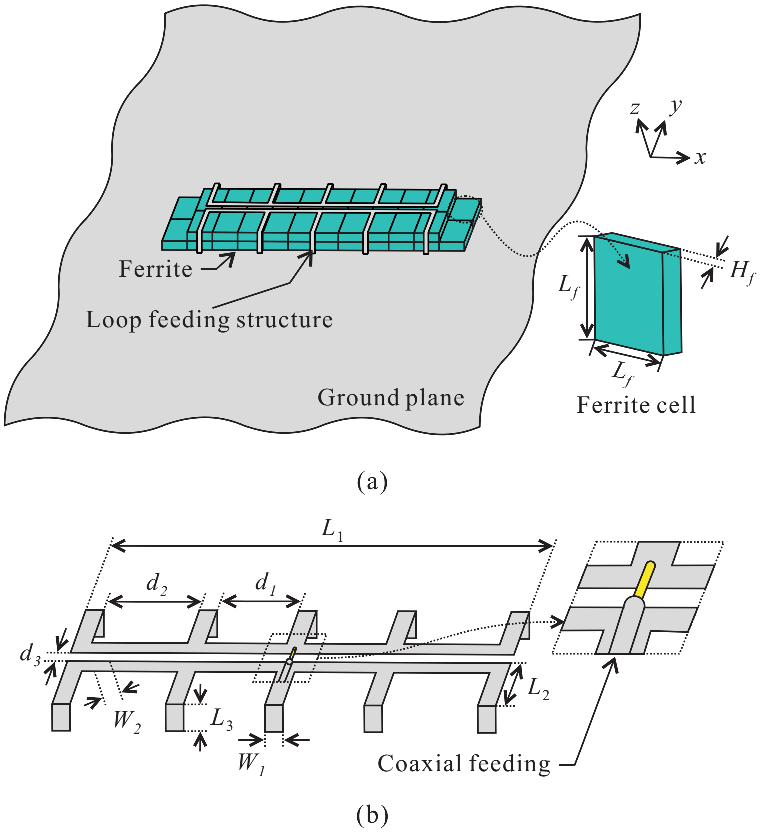

Figure 1. Geometry of the proposed antenna: (**a**) 3-D view and (**b**) feeding structure.

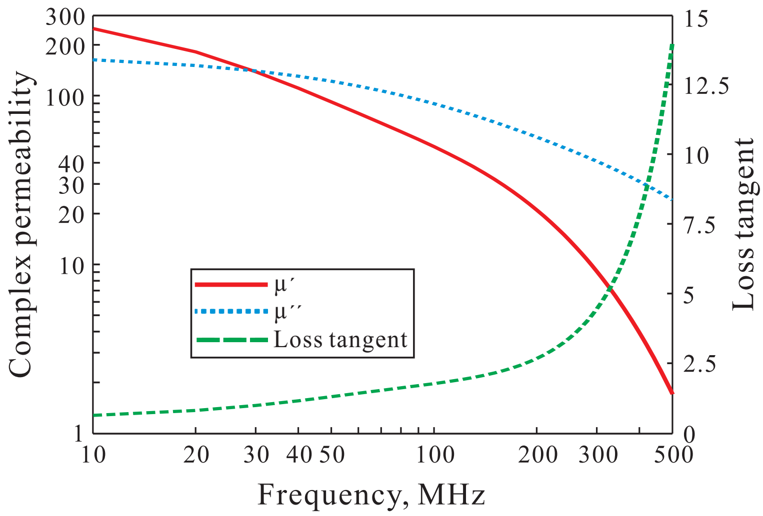

Figure 2. Complex permeability and magnetic loss tangent properties of the MP2106-0M0 ferrite.

To determine how the magnetic field changes with different numbers of loop feeds, the magnetic field distribution around the ferrite dipole at 150 MHz is investigated, as shown in Figure 3, for the 1-loop feed, 3-loop feed, and 5-loop feed. With the 1-loop feed, the loop structure is located at the center of the ferrite dipole structure shown in Figure 3a. For the 3-loop and 5-loop feeds, there is one loop feed structure at the center, and two and four loop feeds are located on the both sides with intervals of d_4 and d_5, respectively. The values of d_4 and d_5 are 159 mm and 106 mm, respectively. In Figure 3b, a strong magnetic field forms around the loop feed structure and rarely extends to the side portions of the ferrite dipole. The magnetic field distribution for the 1-loop feed has a triangular distribution, like the electric field of a small dipole, which results in low radiation efficiency of the antenna. As shown in Figure 3c,d, as the number of loop feeds increases and the magnetic fields become evenly distributed. The 5-loop feed structure is suitable to realize a uniform magnetic field distribution over the entire ferrite dipole, and therefore maximizes the radiation efficiency of the antenna. The simulated magnetic field distributions obtained along the length of the dipole (x-axis) are shown in Figure 3e for the 1-loop feed and 5-loop feed. Clearly, the magnetic field distribution for the 1-loop feed has a triangular distribution while that for the 5-loop feed has a nearly uniform distribution.

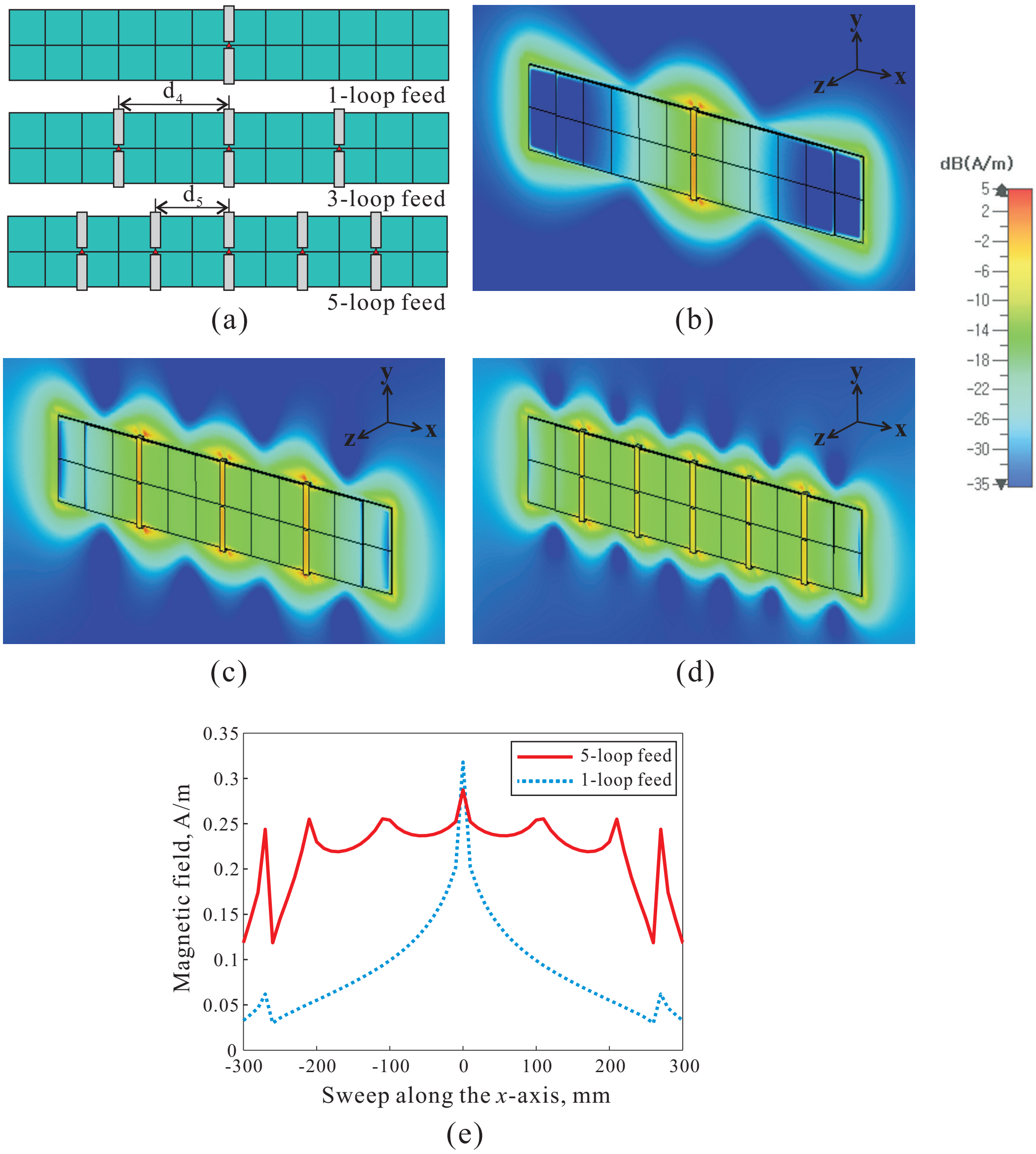

Figure 3. Magnetic field distribution of the ferrite dipole antenna at 150 MHz. (**a**) Geometry of the antenna with different numbers of loop feeds: (**b**) 1-loop feed, (**c**) 3-loop feed, (**d**) and 5-loop feed. (**e**) Simulated magnetic field distribution along the length of the dipole.

Figure 4 plots the simulated realized vertical-polarization gains at the main beam direction ($+z$) for the ferrite dipole antenna on a finite ground plane with a size of 900 mm $\times$ 900 mm with different numbers of loop feeds (see Figure 3a). The gains of the dipole antenna with the 1-loop feed and the 5-loop feed vary from -31.9 to -7.5 dBi and -31 to -1.28 dBi, respectively, in the operating band. Obviously, when the loop feed structure increases, the radiation efficiency of the antenna is increased due to the change in the magnetic field distribution. The gain of the dipole antenna with the 5-loop feed is improved considerably compared to that of the 1-loop feed due to the quasi-uniform magnetic field distribution. The maximum gain improvement is 6.4 dB at 280 MHz. The gain of the dipole antenna with the 5-loop feed is approximately 0.8 dB more than that of the dipole antenna with the 3-loop feed in the middle of its operating band.

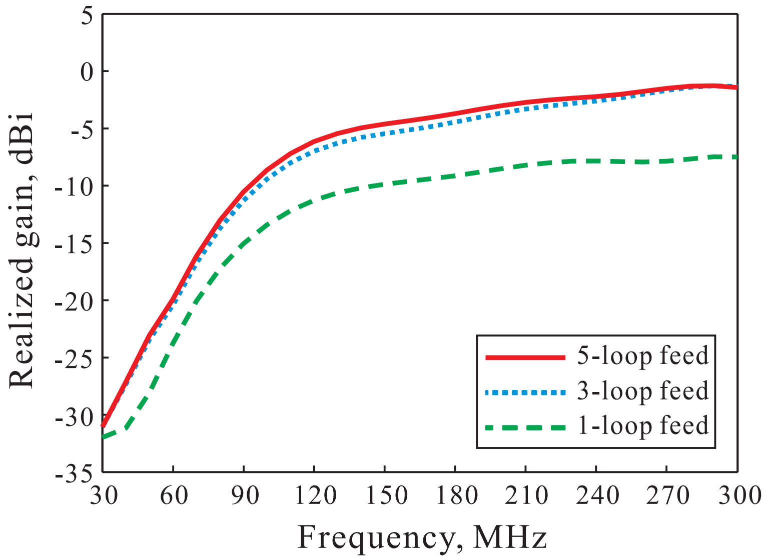

Figure 4. Simulated realized vertical-polarization gains at the main beam direction (+z) of the ferrite dipole antenna with different numbers of loop feeds.

3. Experimental Verification

Based on the optimized design parameters, the proposed antenna was fabricated for an experimental demonstration. Figure 5a shows a photograph of the fabricated antenna. The antenna has a total weight of 1.45 kg and electrical dimensions of approximately $0.0636 \times 0.0112 \times 0.0008\lambda_L^3$ at the lowest operating frequency of 30 MHz. The antenna is mounted at the center of a finite ground plane with a size of 900 mm × 900 mm. The ferrite cells are attached to the ground plane using double-sided tape (see Figure 5b). To simplify the fabrication, the conductor of the loop feeding structure is made of copper tape and is directly attached onto the Styrofoam covering the ferrite dipole structure. The loop feeding structures are connected to the ground plane by silver conductive epoxy (CW2400, Chemtronics). The inner and outer conductors of the coaxial cable are correspondingly connected to the upper and lower arms of the one-quarter rectangular loop, which is placed at the center by soldering. Figure 5c presents a picture of the antenna measurement set-up. Radiation patterns were measured at the outdoor measuring station of the Korea Research Institute of Standards and Science. The proposed antenna was used as a receiving antenna (Rx), and both the transmitting (Tx) and receiving (Rx) antennas are positioned 6 m above the ground.

Figure 6 presents the simulated and measured results of the Voltage Standing Wave Ratio (VSWR) and the realized gains of the proposed antenna. The measurement of the VSWR was done using an Agilent 8510C vector network analyzer. As observed in Figure 6, the simulated and measured results of the VSWR are in good agreement in the entire operating frequency band. The simulated and measured realized gains in the broadside direction ($\theta = 0°$) range from −29.26 to −0.83 dBi and from −31.48 to −2.44 dBi, respectively. The slight discrepancies between the simulated and measured results are mostly caused by fabrication imperfections and/or experimental tolerances due to calibration and reflected and scattered waves from the ground.

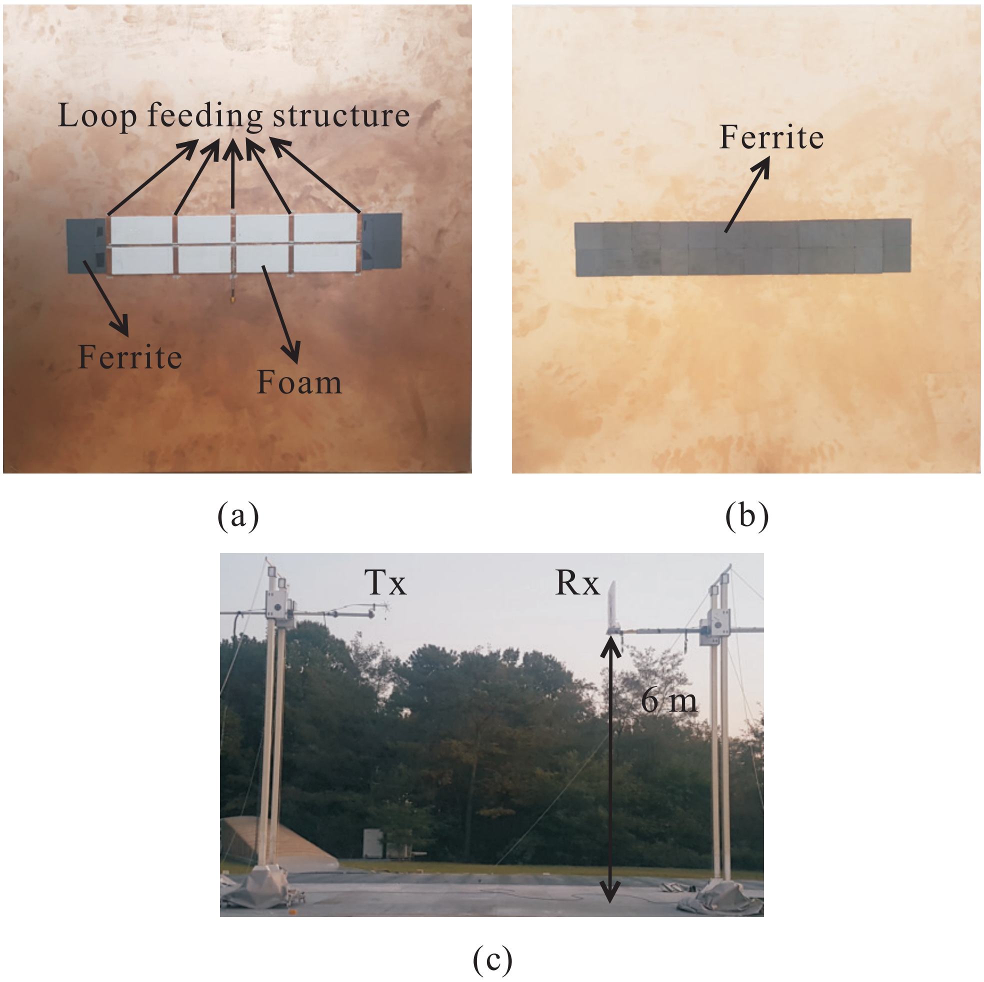

Figure 5. (**a**) Top view of the fabricated proposed antenna. (**b**) Top view of the fabricated ferrite. (**c**) Antenna measurement set-up.

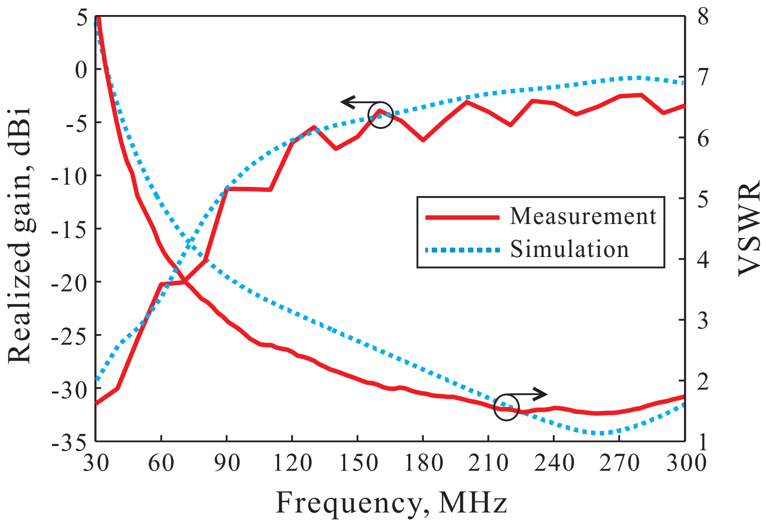

Figure 6. Simulated and measured Voltage Standing Wave Ratios (VSWRs) and realized gains of the proposed antenna.

Table 2 shows a comparison of certain key features between the proposed ferrite dipole antenna and a previous VHF antenna described in the literature [18–20]. Clearly, the antenna presented here has a much lower height and a lighter weight as compared to the antennas reported in earlier studies.

Compared to other designs [18,20], the proposed antenna provides a much higher gain. Although one earlier design [19] has a higher gain, the proposed antenna is smaller and has a much lower height. This makes the proposed antenna an extremely low-profile, lightweight, and high-gain VHF antenna that is very suitable for integrated mast applications.

Table 2. Performance comparison with a previous VHF antenna.

Ref.	Peak Gain (dBi)	Overall Dimensions L×W×H (λ_L^3)	Weight (kg)
[18]	−9	0.04318 × 0.06096 × 0.00508	9.07
[19]	Approx. −0.5	0.1016 × 0.01016 × 0.00381	-
[20]	Approx. −6	0.0381 × 0.0381 × 0.01524	-
This work	−2.44	0.0636 × 0.0112 × 0.0008	1.45

λ_L is the free-space wavelength at the lowest operating frequency of 30 MHz.

Figure 7 shows the simulated and measured radiation patterns at three different frequencies of 30, 100, and 300 MHz on the xz-(ϕ = 0°) and yz-(ϕ = 90°) planes. The dashed and solid lines represent the results of the simulation and the measurement, respectively. The values of the radiation patterns indicate the vertical-polarization gains of the proposed antenna. It can be observed that the proposed antenna radiates omnidirectional and directional waves in the low and high frequency bands, respectively. In addition, the simulated and measured results of the radiation patterns are in good agreement.

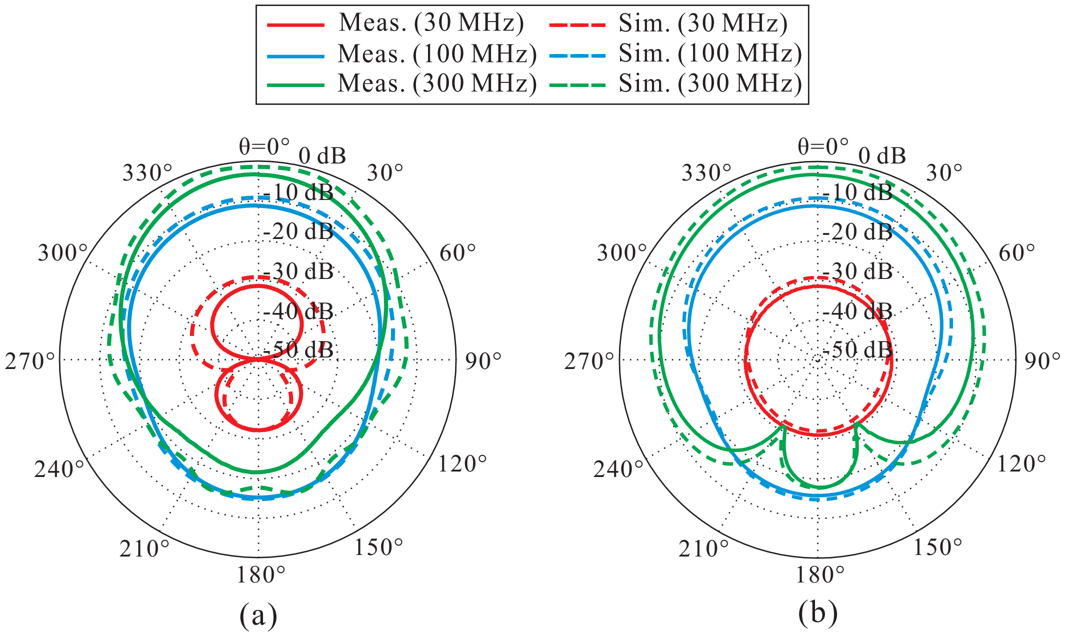

Figure 7. Simulated and measured radiation patterns of the proposed antenna at 30, 100, and 300 MHz: (**a**) xz-plane and (**b**) yz-plane.

Figure 8a shows a photograph of a Holland-class OPV of the Royal Netherland Navy with an integrated mast. To examine the performance of the proposed antenna mounted on the integrated mast in this case, the shape of the OPV is modeled simply (see Figure 8b). The length and beam of the OPV are 108.4 m and 16 m, respectively, and all surfaces are implemented as conductors. The proposed antenna is mounted on the integrated mast of the OPV with vertical (in x-axis) and horizontal (in y-axis) arrangements, as shown in Figure 8c,d, respectively.

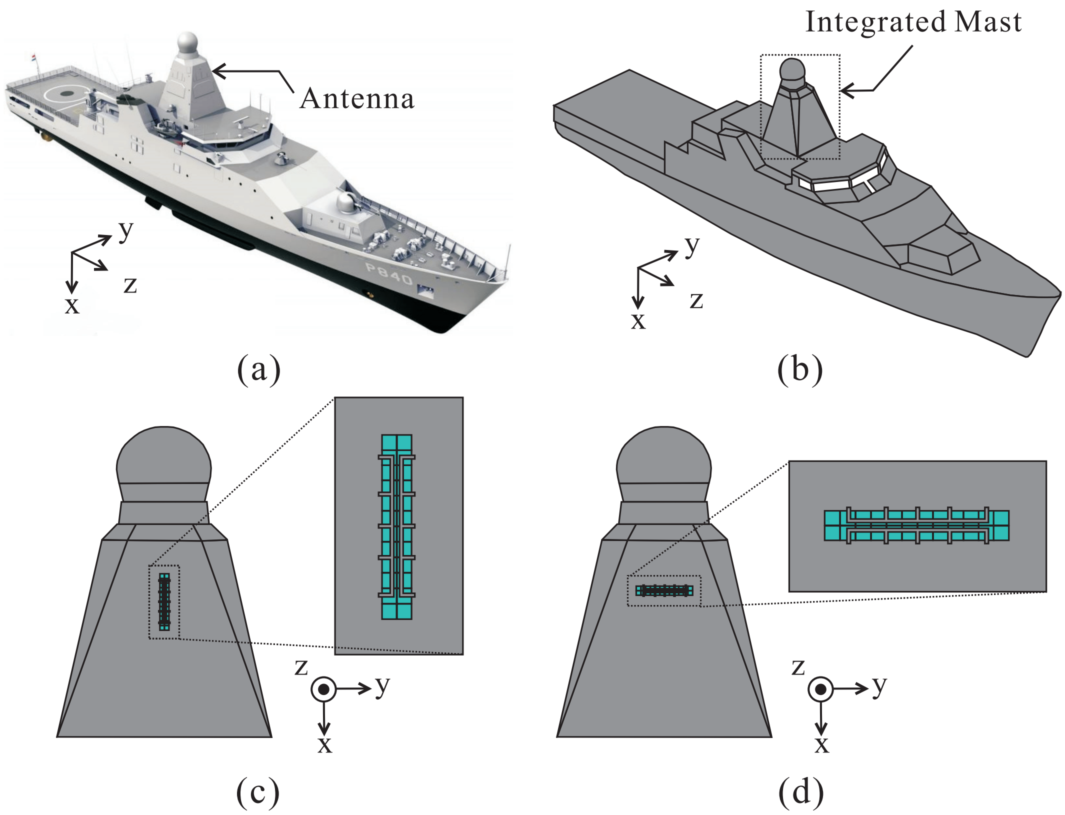

Figure 8. Proposed antenna mounted on the integrated mast of an offshore patrol vessel (OPV): (**a**) Photograph of a Holland-class OPV. (**b**) 3-D modeling of an OPV with the integrated mast. The proposed antenna mounted on the integrated mast of the OPV on the (**c**) x-axis and (**d**) y-axis.

Figure 9 presents the simulated realized gains of the proposed antenna when mounted on the integrated mast of an OPV. The simulated realized gains of the ferrite dipole antenna on the finite flat ground plane (as shown in Figure 6) is also illustrated here as a reference. By mounting the proposed antenna on the integrated mast, the overall structure of the OPV becomes the ground of the antenna. With an integrated mast, the realized gains at low frequencies are higher than that of the proposed antenna due to a significant increase in the size of the ground plane. However, at high frequencies, the realized gains are reduced as compared to that of the proposed antenna. This is mainly due to the electromagnetic waves scattered by the structure of the OPV. The realized gains of the proposed antenna on the integrated mast on the x-axis and y-axis vary from −19.13 to −5.39 dBi and from −17.69 to −4.82 dBi, respectively.

Simulated far-field radiation patterns of the proposed antenna mounted on the integrated mast of an OPV on two cutting planes (xz-plane, yz-plane) are depicted in Figure 10. It can be seen that the radiation patterns are influenced less by the OPV structure at 30 MHz due to the long wavelength; however, when the frequency is increased, the radiation patterns are influenced more by the OPV structure. The xz-plane and yz-plane patterns are directional and omnidirectional patterns, respectively. The proposed antenna is mounted on the front of the integrated mast, and the radiated directional wave is realized in the $+z$-direction. Due to the influence of the bow of the OPV, the directional pattern is tilted toward the $-x$-direction.

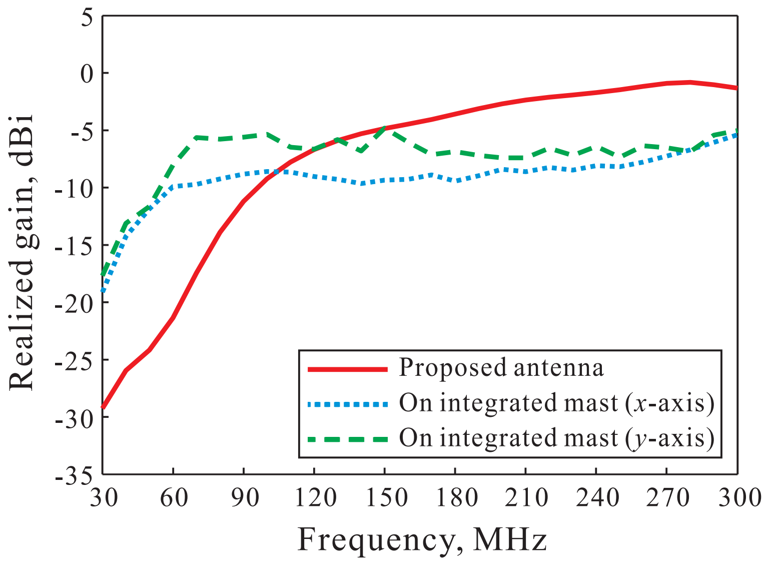

Figure 9. Simulated realized peak gains of the proposed antenna mounted on the integrated mast of an OPV and flat ground conditions.

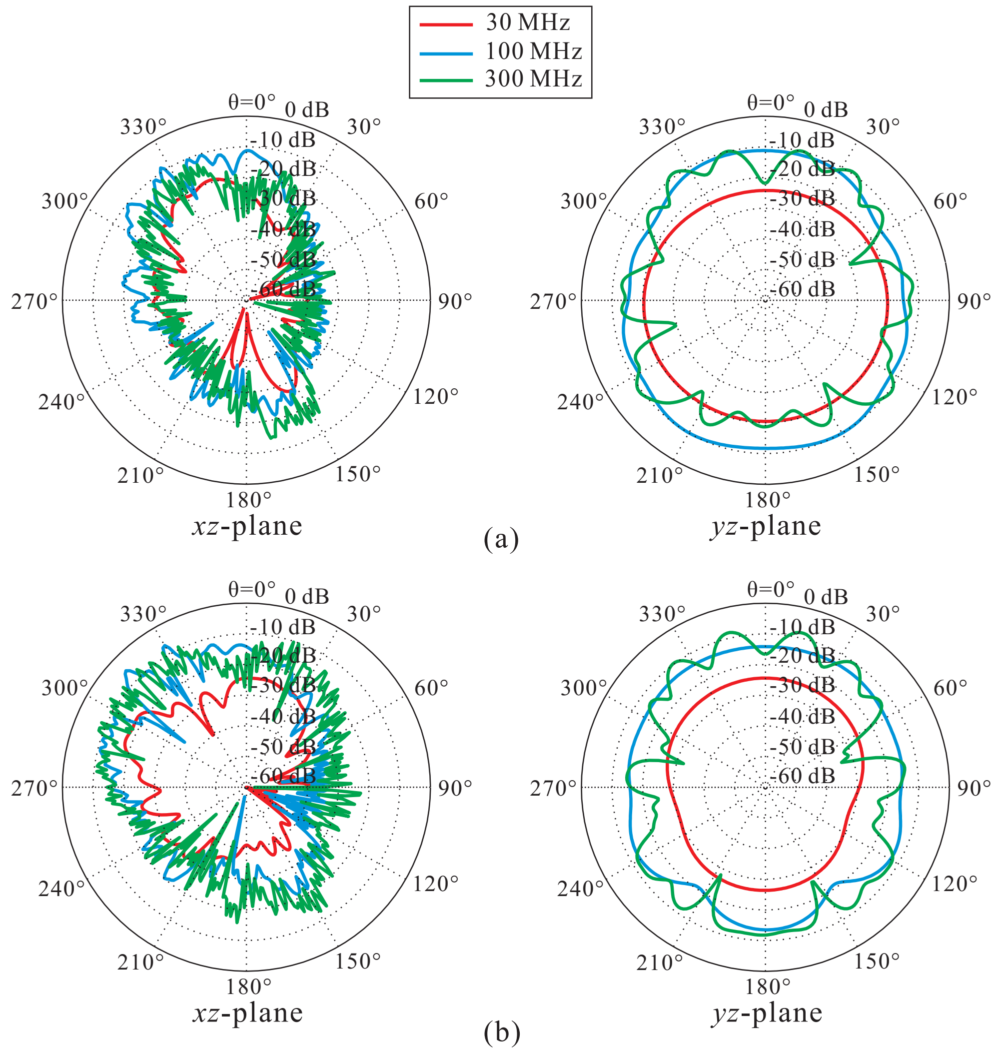

Figure 10. Simulated radiation patterns of the proposed antenna mounted on the integrated mast of an OPV at 30, 100, and 300 MHz: (**a**) x-axis; (**b**) y-axis.

4. Conclusions

An extremely low-profile and lightweight ferrite dipole VHF antenna with a five-loop feed structure was proposed for application to an integrated mast. Ferrite with high permeability was used as the magnetic radiator to ensure low-profile. To consider a proper size and weight of the antenna, the radiator was implemented with only 44 plate-type ferrite cells with an overall weight of 1.45 kg. A multiple-loop feed structure was applied to realize a quasi-uniform magnetic field distribution which enhanced the gain of the antenna over the operating frequency band. Within the VHF band, the measured realized gains of the proposed antenna were from −31.48 to −2.44 dBi. Measured radiation patterns in the low and high frequency bands were omnidirectional and directional, respectively. The performance of the proposed antenna mounted on an OPV was also analyzed. The proposed antenna with overall dimensions of $0.0636 \times 0.0112 \times 0.0008\lambda_L^3$ at the lowest operating frequency shows an extremely low-profile, making it feasible for use as a receiving antenna for integrated mast applications.

Author Contributions: Writing, W.B.P.; Antenna design and simulation, W.B.P. and S.T.-V.; Laboratory tests, W.B.P.; Methodology, Y.Y., K.-Y.L., B.Y., J.P., H.Y. and K.C.H.; Writing Review and Editing, W.B.P., S.T.-V. and K.C.H.; Conceptualization, W.B.P., S.T.-V., Y.Y., K.-Y.L., B.Y., J.P., H.Y. and K.C.H. All authors have read and agreed to the published version of the manuscript.

Funding: This work was supported by a grant-in-aid of HANWHA SYSTEMS.

Conflicts of Interest: The authors declare no conflicts of interest.

References

1. Van Werkhoven, G.H.C.; Van Aken, R.H. Evolutions in naval phased array radar at Thales Nederland B.V. In Proceedings of the Fourth European Conference on Antennas and Propagation, Barcelona, Spain, 12–16 April 2010.
2. Bijman, R.; Timens, R.B.; Leferink, F. Effect of integrated mast on power quality of naval vessel in island configuration. In Proceedings of the 2013 International Symposium on Electromagnetic Compatibility, Brugge, Belgium, 2–6 September 2013.
3. Cheng, X.; Yan, H.; Hu, Y. Electromagnetic interference analysis of integrated radar antennas on stealth mast. In Proceedings of the 2015 7th Asia-Pacific Conference on Environmental Electromagnetics, Hangzhou, China, 4–7 November 2015.
4. Cifola, L.; Gerini, G.; Monni, S.; Van den Berg, S.;Van de Water, F. Integrated filtering in reconfigurable planar phased-array antennas with spurious harmonic suppression. In Proceedings of the 2013 IEEE International Symposium on Phased Array Systems and Technology, Waltham, MA, USA, 15–18 Octorber 2013.
5. Lin, B.; Li, F.; Zheng, Q.; Zen, Y. Design and simulation of a miniature thick-screen frequency selective surface radome. *IEEE Antennas Wirel. Propag. Lett.* **2009**, *8*, 1065–1068.
6. Chen, H.; Hou, X.; Deng, L. Design of frequency-selective surfaces radome for a planar slotted waveguide antenna. *IEEE Antennas Wirel. Propag. Lett.* **2009**, *8*, 1231–1233. [CrossRef]
7. Mattioni, L.; Marrocco, G. Design of a broadband HF antenna for multimode naval communications. *IEEE Antennas Wirel. Propag. Lett.* **2005**, *4*, 179–182. [CrossRef]
8. Marrocco, G.; Mattioni, L. Naval structural antenna systems for broadband HF communications. *IEEE Trans. Antennas Propag.* **2006**, *54*, 1065–1073. [CrossRef]
9. Wang, C.; Yuan, B.; Mao, J.; Shi, W. Dual-sleeve wideband monopole antenna for shipborne systems in VHF band. *Electron. Lett.* **2018**, *54*, 1102–1104. [CrossRef]
10. Jacobsen, R.E.; Lavrinenko, A.V.; Arslanagiv, S. Electrically small water-based hemispherical dielectric resonator antenna. *Appl. Sci.* **2019**, *9*, 4848. [CrossRef]
11. Kedze, K.E.; Wang, H.; Park, I. Effects of split position on the performance of a compact broadband printed dipole antenna with split-ring resonators. *J. Electromagn. Eng. Sci.* **2019**, *19*, 115–121. [CrossRef]
12. Kothapudi, V.K.; Kumar, V. SFCFOS uniform and chebyshev amplitude distribution linear array antenna for K-Band Applications. *J. Electromagn. Eng. Sci.* **2019**, *19*, 64–70. [CrossRef]

13. Yoon, S.J.; Choi, J. A low-profile broadband array antenna for home repeater applications. *J. Electromagn. Eng. Sci.* **2018**, *18*, 261–266. [CrossRef]
14. Kim, J.-H.; Kim, B.-G. Effect of feed substrate thickness on the bandwidth and radiation characteristics of an aperture-coupled microstrip antenna with a high permittivity feed substrate. *J. Electromagn. Eng. Sci.* **2018**, *18*, 101–107. [CrossRef]
15. Keum, K.; Piao, H.; Choi, J. Design of a short/open-ended slot antenna with capacitive coupling feed strips for hepta-band mobile application. *J. Electromagn. Eng. Sci.* **2018**, *18*, 46–51. [CrossRef]
16. Ghaemi, K.; Behdad, N. A Low-Profile, Wideband antenna with vertically polarized directional radiation. *IEEE Antennas Wirel. Propag. Lett.* **2016**, *15*, 1093–1096. [CrossRef]
17. Abadi, S.M.A.M.H.; Behdad, N. An electrically small, vertically polarized ultrawideband antenna with monopole-like radiation characteristics. *IEEE Antennas Wirel. Propag. Lett.* **2014**, *13*, 742–745. [CrossRef]
18. Moon, H.; Lee, G.; Chen, C.; Volakis, J.L. An extremely low-profile ferrite-loaded wideband VHF antenna design. *IEEE Antennas Wirel. Propag. Lett.* **2012**, *11*, 322–325. [CrossRef]
19. Yousefi, T.; Sebastian, T.; Diaz, R.E. Why the magnetic loss tangent is not a relevant constraint for permeable conformal antennas. *IEEE Trans. Antennas Propag.* **2016**, *64*, 2784–2796. [CrossRef]
20. Osaretin, I.A.; Torres, A.; Chen, C. A novel compact dual-linear polarized UWB antenna for VHF/UHF applications. *IEEE Antennas Wirel. Propag. Lett.* **2009**, *8*, 145–148. [CrossRef]
21. MP2106-0M0. Available online: https://www.mouser.com/datasheet/2/987/MP2106-0M0-1650723.pdf (accessed on 17 December 2019)